CHIN. PHYS. LETT. Vol. 35, No. 7 (2018) 074204

Field Tunable Polaritonic Band Gaps in Fibonacci Piezoelectric Superlattices *

Zheng-Hua Tang(唐政华)[1], Zheng-Sheng Jiang(蒋正生)[2], Chun-Zhi Jiang(蒋纯志)[1**], Da-Jun Lei(雷大军)[1], Jian-Quan Huang(黄健全)[1], Feng Qiu(邱枫)[1], Hai-Ming Deng(邓海明)[1], Min Yao(姚敏)[1], Xiao-Yi Huang(黄小益)[1]

[1]*Xiangnan University-Gospell Joint laboratory of Microwave Communication Technology, college of Electronic Information and Electrical Engineering, Xiangnan University, Chenzhou 423000*

[2]*National Laboratory of Solid State Microstructures and Department of Physics, Nanjing University, Nanjing 210093*

(Received 23 April 2018)

The Fibonacci piezoelectric superlattices (FPSs) with an external dc electric field is presented, in which the dc electric field can tune the bandwidth of polaritonic band gaps (PBGs) continuously and reversibly via the electro-optic effect. The absolute bandwidths of two major PBGs of the FPSs around $\omega = 7.5$ GHz and $\omega = 12.5$ GHz can be broadened from 0.022 GHz to 0.74 GHz and from 0.02 GHz to 0.82 GHz with the dc electric field increasing from 0 to 1.342×10^6 V/m, respectively. The corresponding relative bandwidths of the two major PBGs are widened from 0.28% to 9.2% and from 0.18% to 6.35%, respectively. The general mechanism for the bandwidth tunability is that the coupling strength between the lattice vibration and electromagnetic waves is capable of being altered by the dc electric field via the electro-optic effect. Thus the properties can be applied to construct microwave switchings or field tunable bulk acoustic filters.

PACS: 42.25.Bs, 71.36.+c, 77.65.−j DOI: 10.1088/0256-307X/35/7/074204

Phonon polaritons have received increasing attention in recent years because of their applications in different types of polaritonic devices such as waveguides, resonators, and gratings.[1] The phonon polaritons in piezoelectric or piezomagnetic superlattices originate from the electromagnetic wave-lattice vibration coupling,[2] and the transfer matrix method[3–5] is utilized to compute accurately polaritonic band structures and transmission spectra. The coupling of electromagnetic waves to surface acoustic waves can also cause the surface phonon polaritons[6–8] on piezoelectric superlattices to be generated. Currently, a variety of experimental designs[9–14] with respect to phonon polaritons have been investigated and many properties[15–18] associated with the phonon polaritons are discussed. An optical isolator can be tuned by altering the external dc electric field via the electro-optic effect[19] and the photonic band gaps can be tuned by changing the temperature.[20]

From the above comprehensive understanding, although there have been many investigations on the PBGs so far, the research regarding the tunability of the PBGs of the FPSs via the electro-optic effect, especially in the microwave frequency range, is still rare. As the experimental configuration illustrated in Fig. 1, the ferroelectric domains with polarization along the $\pm z$ axis are marked as B and A, respectively. The formula $S_l = S_{l-2}S_{l-1}$ for $l \geq 2$, with S_0=B and S_1=A, is used to define the stacking rule of the Fibonacci sequences, and S_l denotes the lth generational sequence. Here F_l is the number of layers and follows the rule of iteration $F_l = F_{l-1} + F_{l-2}$, with $F_1 = F_0 = 1$. The Fibonacci piezoelectric superlattices are constructed by arranging the domains B and A according to the rule mentioned above and an applied direct-current (dc) electric field along the $+z$ axis is implemented on themselves. Three key points with regard to the FPSs under the dc electric field need to be emphasized, as follows: (1) the relative bandwidths of mainly PBGs around $\omega = 7.5$ GHz and $\omega = 12.5$ GHz are altered from 0.28% to 9.2% and from 0.18% to 6.3% for the structure with $L_{P+} = L_{P-} = 1.38\,\mu$m when the dc electric field is increased from $E_z^0 = 0$ to 1.342×10^6 V/m, respectively. (2) The four minor PBGs around $\omega = 4.7$, 9.5, 10.5 and 15.2 GHz are opened for this structure under the electric field of $E_z^0 = 1.342 \times 10^6$ V/m though they do not exist in the absence of the dc electric field. (3) The bandwidth tunability of multi-channel band gaps of the FPSs by an external dc electric field via the electro-optic effect is synchronous and reversible.

In this study, the FPSs with the Fibonacci sequence S_5 (8 layers) as shown in Fig. 1 can be treated as a one-dimensional structure due to its longitudinal dimension is larger than that of its transverse. An external dc electric field along the z-axis applied on the FPSs is to ensure that the adjustment of the electro-optic effect for the experimental setting can occur. Owing to complete material parameters,[21] the large electro-optic coefficient[22] and the high coercive field[23] available, a ferroelectric PZT compound is selected as the candidate material of the piezoelectric

*Supported by the National Natural Science Foundation of China under Grant No 11705155, the Science and Technology Innovative Research Team in Higher Educational Institutions of Hunan Province, the Projects of Hunan Provincial Education Office under Grant Nos 16B243, 17B244 and 16A199, and the Chenzhou City Science and Technology Project under Grant Nos CZ2014042 and jsyf2017005.

**Corresponding author. Email: jiangchunzhi1213@sina.com

© 2018 Chinese Physical Society and IOP Publishing Ltd

domains. As in the situation in Fig. 1, the polarization of piezoelectric domains of the FPSs is along the $\pm z$-axis and $L = L_{P+} + L_{P-}$ is the lattice period, with L_{P+} and L_{P-} denoting the layer thicknesses of A and B domains, respectively. Such choices ensure that the bandwidth of PBGs can be adjusted freely by an external dc field via the electro-optic effect when electromagnetic waves propagate along the structure. Considering an electromagnetic wave impinging on the FPSs, the electromagnetic wave can couple to the longitudinal acoustic wave.

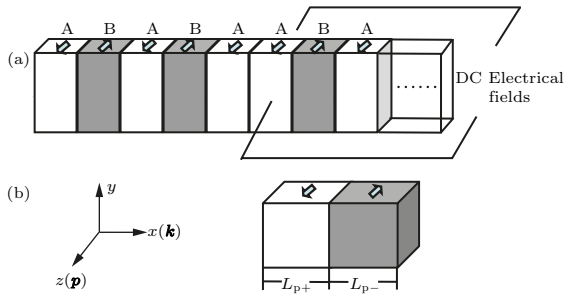

Fig. 1. A schematic diagram of the Fibonacci piezoelectric superlattices with an external dc electric field along the z-axis (a) and of A and B domains (b). L_{P+} and L_{P-} denote the thicknesses of A and B domains, which are set as $L_{P+} = L_{P-} = 1.38\,\mu$m. The white and gray blocks represent the piezoelectric domains with polarization along the $\pm z$-axis, respectively. The wavevector k is along the x-axis.

For a transverse-electric-magnetic (TEM) plane wave passing through the FPSs, the dynamic equations among longitudinal lattice displacement $u_x(x,t)$, transverse electric field $E_y(x,t)$ and transverse magnetic field $H_y(x,t)$ can be written as

$$\left(\frac{\omega L}{2\pi c_{\rm s}}\right)\bar{E}_z(\bar{x},\omega) = i\alpha_1\frac{\partial}{\partial\bar{x}}\bar{H}_y(\bar{x},\omega) + \beta_1\left(\frac{\omega L}{2\pi c_{\rm s}}\right)\theta(\bar{x})\frac{\partial}{\partial\bar{x}}\bar{u}_x(\bar{x},\omega), \quad (1)$$

$$\left(\frac{\omega L}{2\pi c_{\rm s}}\right)\bar{H}_y(\bar{x},\omega) = i\alpha_2\frac{\partial}{\partial\bar{x}}\bar{E}_z(\bar{x},\omega), \quad (2)$$

$$\left(\frac{\omega L}{2\pi c_{\rm s}}\right)^2\bar{u}_x(\bar{x},\omega) = -\frac{\partial^2}{\partial\bar{x}^2}\bar{u}_x(\bar{x},\omega) + \frac{\partial}{\partial\bar{x}}[\theta(\bar{x})\bar{E}_z(\bar{x},\omega)]. \quad (3)$$

The dynamical properties for electromagnetic waves propagating in the FPSs can be described by the dimensionless equations mentioned above. Here ω indicates the frequency of the incident electromagnetic wave, L is the sum of A and B domains, $c_{\rm s} = \sqrt{\bar{K}_{11}/\rho}$ is the sound velocity of the ferroelectric PZT compound, ρ denotes its density, and K_{ij} $(i,j = 1,2,3)$ denotes the reduced bulk modulus and is defined as the inverse matrix of the elastic compliance tensor. The dimensionless form of Eqs. (1)–(3) can be derived by introducing the dimensionless variable $x = \bar{x}L/2\pi$ and dimensionless functions $\bar{H}_y(x,t) = \sqrt{\mu_0/\bar{K}_{11}}H_y(x,t)$, $u_x(x,t) = \bar{u}_x(x,t)L/2\pi$, $\bar{E}_z(x,t) = \bar{d}_{31}(\bar{x})E_z(x,t)$ and can facilitate the calculation, where μ_0 is the magnetic permeability in a vacuum, $\bar{d}_{31}(x) = [d(x)K]_{31}/K_{11}$ represents the effective piezoelectric coefficient, $\bar{d}_{31}(\bar{x}) = \bar{d}_{31}\theta(\bar{x})$ is introduced to describe the polarization direction, the step-function $\theta(\bar{x}) = \pm 1$ denotes the domains with polarization along the $\pm z$ axis, and $\alpha_1 = \bar{d}_{31}/\epsilon_0\bar{\epsilon}c_{\rm s}\sqrt{\mu_0/K_{11}}$ and $\alpha_2 = 1/\bar{d}_{31}c_{\rm s}\sqrt{\mu_0 K_{11}}$ are the dimensionless coefficients of Eqs. (1)–(3). The conversion efficiency between the electrical energy and the mechanic energy in the FPSs is characterized by the electromechanical coefficient $\beta_1 = K_{11}\bar{d}_{31}^2/\epsilon_0\bar{\epsilon}$. It reflects the coupling strength between electromagnetic waves and the lattice displacement via the piezoelectric effect. Here $\bar{\epsilon} = \epsilon_{33} - \Delta\epsilon_{33} - \gamma_{33}\epsilon_{33}^2E_z^0$ denotes the reduced dielectric constant, ϵ_{33} is the relative permittivity, $\Delta\epsilon_{33} = (dKd^T)_{33}/\epsilon_0$ is the correction to the dielectric constant from the electromechanical effect, $\gamma_{33}\epsilon_{33}^2E_z^0$ is the correction of dielectric constant emanating from the electro-optic effect, γ_{33} is the electro-optic coefficient, and E_z^0 denotes the dc electric field along the z-axis.

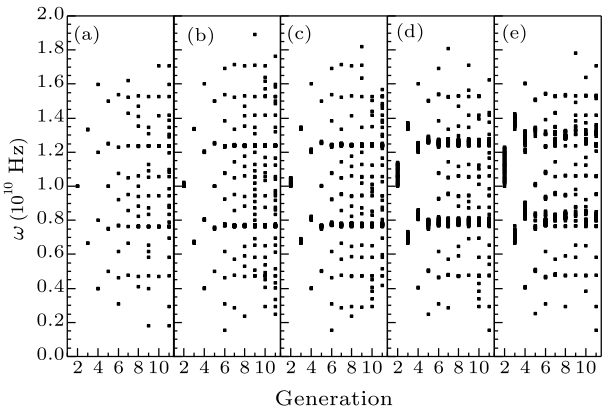

Fig. 2. The evolutionary relationship of polaritonic band gaps at different dc electric fields of (a) $E_z^0 = 0\,$V/m, (b) $E_z^0 = 1.248\times10^6\,$V/m, (c) $E_z^0 = 1.306\times10^6\,$V/m, (d) $E_z^0 = 1.335\times10^6\,$V/m and (e) $E_z^0 = 1.342\times10^6\,$V/m with the Fibonacci generation $l = 2$–10. The reduced domain thicknesses are the same as in Fig. 1.

The complete material parameters and the large electro-optic coefficient of the ferroelectric compound PZT can be obtained from Ref. [22]. The dimensionless coefficients $\alpha_1 = 110.95$, $\alpha_2 = 7.28\times10^9$ and $\beta = 0.004$ of Eqs. (1)–(3) can be derived easily in the absence of the external dc electric field by substituting the material parameters of PZT. The value of the dimensionless parameter β indicates that the electro-mechanic coefficient is so weak in the FPSs that the influence of the piezoelectric effect on the bandwidth of the PBGs is not remarkable. On the contrary, it is conducive for the electro-optic effect in the FPSs to play the dominant role in manipulating the PBGs. The domain thickness of the FPSs is $L_{p+} = L_{p-} = 1.38\,\mu$m. Combining the above parameters, the coupled polaritonic band structures of the FPSs can be calculated and shown in Fig. 2.

The generation of the coupled polaritonic band structures can be described by a three-step process: (1) the periodical modulation of the piezoelectric coefficient can induce the acoustic dispersion relation to be folded; (2) the folded branches of acoustic dispersion relation intersecting with electromagnetic waves' dispersion branches can open the PBGs; (3) the bandwidths of the PBGs can be adjusted by the external dc electric field via the electro-optic effect. The vertical and horizontal axes represent the frequency and the generation l, respectively. The values of the external dc electric field of the FPSs are chosen as $E_z^0 = 0$, 1.248×10^6 V/m, 1.306×10^6 V/m, 1.335×10^6 V/m and 1.342×10^6 V/m and the coupled polaritonic band structures for the FPSs can be calculated by the transfer matrix method, shown in Fig. 2(a)–2(e), respectively.

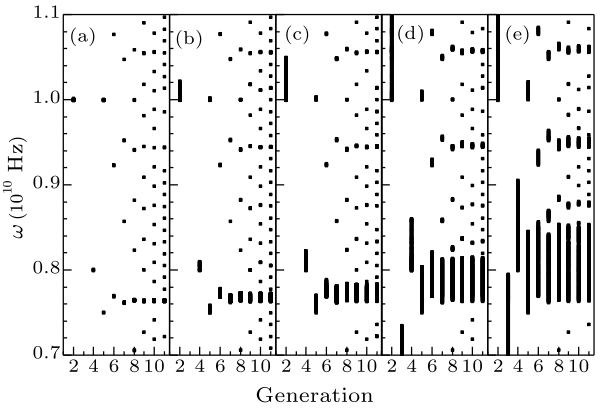

Fig. 3. The polaritonic band gaps of $\omega = 7.0$–11.0 GHz at the same dc electric fields as in Fig. 2. The reduced domain thicknesses are the same as in Fig. 1.

The polarization of piezoelectric domains of the FPSs remains unchanged due to the fact that the value of the coercive field (7.0×10^6 V/m)[23] of PZT is much larger than that of the external dc electric field. The solid squares in Fig. 2 represent the polaritonic band gaps. The propagating of electromagnetic waves within the PBGs will be prohibited, otherwise, they can travel along the FPSs. Two major PBGs for electromagnetic waves can be observed around $\omega = 7.5$ GHz and $\omega = 12.5$ GHz and four minor PBGs of the FPSs occur in the vicinity of $\omega = 4.7$, 9.5, 10.5 and 15.2 GHz. To observe the PBGs clearly, the coupled polaritonic band structures around $\omega = 7.5$ GHz under the dc electric fields of $E_z^0 = 0$, 1.248×10^6, 1.306×10^6, 1.335×10^6 and 1.342×10^6 V/m are enlarged and replotted in Figs. 3(a)–3(e), respectively. From Figs. 3(a)–3(e), we can easily conclude that the width of the solid squares will be significantly widened when the external dc electric fields are increased from 0 to 1.342×10^6 V/m. This means that the pass band of electromagnetic waves around $\omega = 7.5$ GHz in Fig. 3(a) will be converted into the forbidden band as a result of the dc electric field increasing, which are consistent with the transmission spectrum mentioned in Fig. 4.

To further check the coupled polaritonic band structures of the FPSs under the different dc electric fields, the transmission spectra for the FPSs with the total layers of $S_{23} = 46368$ (0.128 m) are computed and illustrated in Figs. 4 and 5, respectively. No obvious PBGs can be observed in Fig. 4(a) due to the relatively weak electro-mechanic coefficient. Two major PBGs around $\omega = 7.5$ GHz and $\omega = 12.5$ GHz in Figs. 4(b)–4(e) are labeled as gaps 1 and 2. If the incident electromagnetic waves fall within the PBGs, they will be greatly attenuated by the FPSs. As the dc electric fields are varied from $E_z^0 = 0$ V, 1.248×10^6, 1.306×10^6, 1.335×10^6 to 1.342×10^6 V/m, the relative bandwidths of gap 1 are up to 0.28%, 1.29%, 2.28%, 5.33% and 9.2% and of gap 2 are 0.18%, 0.6%, 1.24%, 3.14% and 6.35%, respectively. The corresponding maximum absolute bandwidths of gaps 1 and 2 under the dc electric field $E_z^0 = 1.342 \times 10^6$ V/m as shown in Fig. 4(e) can reach 0.74 GHz and 0.82 GHz, respectively. The other four minor PBGs around $\omega = 4.7$, 9.5, 10.5 and 15.2 GHz occur in Fig. 4(e) and the relative bandwidths for them are 1.16%, 0.8%, 0.6% and 0.5%, and the absolute bandwidths for them are 0.055, 0.077, 0.066, 0.077 GHz, respectively. As in the situation shown in Fig. 4(a), these minor PBGs may not exist because of the lack of the dc electric field. Owing to the values of the external dc electric field being less than those of the coercive field, the external dc electric field cannot break the polarization of piezoelectric domains of the FPSs. Thus the structure can maintain stability under the action of the external electric field.

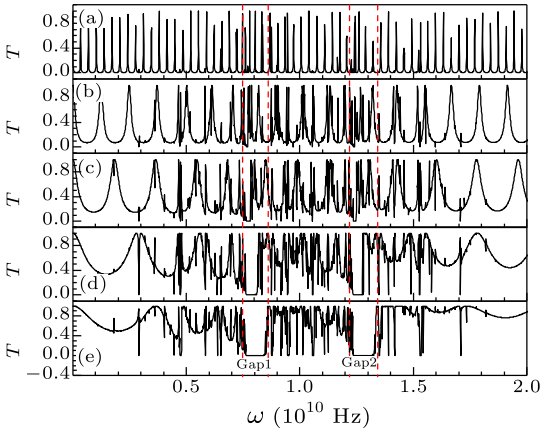

Fig. 4. The transmission spectra at the same dc electric fields as in Fig. 2 for the FPSs with the total periods of 46368 (0.128 m). The reduced domain thicknesses are the same as in Fig. 1.

To further describe the relationship between the bandwidths of the PBGs and the external dc electric field, the coupled polaritonic band structures around gap 1 in Fig. 4 are enlarged and replotted in Fig. 5. From Figs. 5(b)–5(e), the lower band edges of the PBGs remain unchanged and are approximately 7.58 GHz, and the upper band edges of the PBGs

are varied from 7.7, 7.8, 8.2 to 8.5 GHz. The bandwidth of the PBGs can be adjusted by the external dc electric field, and the FPSs with the external electric field show a microwave switching effect. The bandwidth modulation method of the FPSs does not need to change the size of the structure or to reconstruct structural elements. The only necessary means for adjusting the bandwidth of the PBGs is to vary the intensity of the external dc electric field. An increase in the dc electric field intension will widen the bandwidth of the PBGs to a certain extent and a decrease in the dc electric field will correspondingly narrow the bandwidth of the PBGs. Thus the FPSs with the external dc electric field exhibit a quite good electrical tunability and the adjustment of the bandwidth of the PBGs by an external dc electric field is continuous and reversible, and of all the PBGs are synchronous. Essentially, the coupling interaction between electromagnetic waves and the lattice vibration of the FPSs can be strengthened by the applied dc electric field via the electro-optic effect. This can improve the electromechanical effect and further increase the bandwidth of the PBGs of the FPSs.

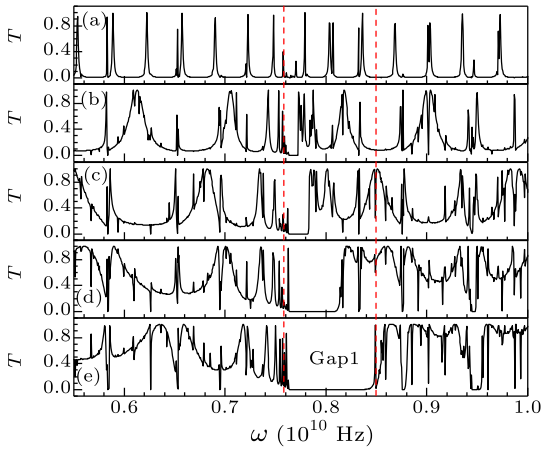

Fig. 5. The transmission spectra of $\omega = 5.5$–10.0 GHz at the same dc electric fields as in Fig. 2 for the FPSs with the total periods of 46368 (0.128 m). The reduced domain thicknesses are the same as in Fig. 1.

Extensive discussions regarding the Fibonacci piezoelectric superlattices have been carried out in Ref. [4]. The band structures of the FPSs indicate that a self-similar pattern can be observed for the spectra differing by three generations, and the transmission spectra of the FPSs display the multi-channel PBGs. The multi-channel PBGs of the FPSs can be tuned by the external dc electric field via the electro-optic effect. Thus the FPSs under the action of the external dc electric field shown in Fig. 1 also contains the essential ingredients for constructing the multi-channel microwave switching due to its tunable PBGs by the dc electric field.

In summary, the experimental design in this work contains the Fibonacci piezoelectric superlattices with the external dc electric field along the z-axis. The coupled polaritonic band structures and the transmission spectra of the FPSs show clearly that the bandwidth of the PBGs can be tuned by the dc electric field via the electro-optic effect. Therefore, the FPSs can be utilized to construct novel microwave switchings or field tunable bulk acoustic filters.

References

[1] Lee Y S 2009 *Principles Terahertz Sci. Technol.* (Berlin: Springer) chap 5 p 211
[2] Lu Y Q, Zhu Y Y, Chen Y F, Zhu S N, Ming N B and Feng Y J 1999 *Science* **284** 1822
[3] Zhang W Y, Liu Z X and Wang Z L 2005 *Phys. Rev.* B **71** 195114
[4] Liu Z X and Zhang W Y 2005 *Phys. Rev.* B **72** 134304
[5] Liu Z X and Zhang W Y 2007 *Phys. Rev.* B **75** 064207
[6] Hu X K, Ming Y, Zhang X J, Lu Y Q and Zhu Y Y 2012 *Appl. Phys. Lett.* **101** 151109
[7] Yudistira D, Boes A, Djafari-Rouhani B, Pennec Y, Yeo L Y, Mitchell A and Friend J R 2014 *Phys. Rev. Lett.* **113** 215503
[8] Ng S S, Hassan Z and Abu H 2008 *Chin. Phys. Lett.* **25** 4378
[9] Devarapu G C R and Foteinopoulou S 2017 *Phys. Rev. Appl.* **7** 034001
[10] Sakamoto H, Takeuchi E, Yoshida K, Morita K, Ma B and Ishitani Y 2018 *J. Phys.* D **51** 015105
[11] Karakachian H and Kazan M 2017 *J. Appl. Phys.* **122** 045103
[12] Feng K J, Streyer W, Islam S M, Verma J, Jena D, Wasserman D and Hoffman A 2015 *Appl. Phys. Lett.* **107** 081108
[13] Müler K, Fischer K A, Rundquist A, Dory C, Lagoudakis K G, Sarmiento T, Kelaita Y A, Borish V and Vučković 2015 *Phys. Rev.* X **5** 031006
[14] Ikegaya Y, Sakaibara H, Minami Y, Katayama I and Takeda J 2015 *Appl. Phys. Lett.* **107** 062901
[15] Chen K F, Santhanam P and Fan S H 2015 *Appl. Phys. Lett.* **107** 091106
[16] Kojima S and Mori T 2016 *Ferroelectrics* **500** 183
[17] Ordonez-Miranda J, Tranchant L, Joulain K, Ezzahri Y, Drevillon J and Volz S 2016 *Phys. Rev.* B **93** 035428
[18] Janipour M, Misirlioglu I B and Sendur K 2016 *Sci. Rep.* **6** 34071
[19] Qian X S, Wu H, Wang Q, Yu Z Y, Xu F, Lu Y Q and Chen Y F 2011 *J. Appl. Phys.* **109** 053111
[20] Ramanujama N R and Joseph W K S 2017 *Opt. Commun.* **386** 65
[21] Bichurin M I and Petrov V M 2003 *Phys. Rev.* B **68** 054402
[22] Kang T D, Xiao B, Avrutin V, Özgür Ü, Morkoc H, Park J W, Lee H S, Wang X Y and Smith D J 2008 *J. Appl. Phys.* **104** 093103
[23] George J P, Smet P F, Botterman J, Bliznuk V, Woestenborghs W, Thourhout D V, Neyts K and Beeckman J 2015 *ACS Appl. Mater. Interfaces* **7** 13350